Collective circular motion of multi-vehicle systems with sensory limitations

Nicola Ceccarelli, Mauro Di Marco, Andrea Garulli, Antonello Giannitrapani

Dipartimento di Ingegneria dell'Informazione
Università di Siena
Via Roma 56, 53100 Siena, Italy
ceccarelli,dimarco,garulli,giannitrapani@dii.unisi.it

***Abstract*— Collective motion of a multi-agent system composed of nonholonomic vehicles is addressed. The aim of the vehicles is to achieve rotational motion around a virtual reference beacon. A control law is proposed, which guarantees global asymptotic stability of the circular motion with a prescribed direction of rotation, in the case of a single vehicle. Equilibrium configurations of the multi-vehicle system are studied and sufficient conditions for their local stability are given, in terms of the control law design parameters. Practical issues related to sensory limitations are taken into account. The transient behavior of the multi-vehicle system is analyzed via numerical simulations.**

I. Introduction

Multi-agent systems have received an increased interest in recent years, due to their enormous potential in several fields: collective motion of autonomous vehicles, exploration of unknown environments, surveillance, distributed sensor networks, biology, etc. (see e.g. [1], [2] and references therein). Although a rigorous stability analysis of multi-agent systems is generally a very difficult task, nice theoretical results have been obtained in the case of linear motion models. One of the first contributions in this respect was given in [3], where a multi-vehicle system with a virtual reference beacon is considered. Leader following, leaderless coordination and cyclic pursuits have been studied in [1], [4]. Stability analysis becomes even more challenging when kinematic constraints are taken into account, as in the case of wheeled nonholonomic vehicles. Unicycle-like motion models have been recently considered in several papers [5], [6], [2], [7]. In particular, in [6], [5], [7] different control laws are proposed for circular and parallel motion of planar multi-vehicle systems, with complete stability analysis of the single-vehicle case. In [2], equilibrium formations of multi-vehicle systems in cyclic pursuit are studied, and local stability is discussed in detail.

In this paper, the objective of a team of nonholonomic vehicles is to achieve collective circular motion around a virtual reference beacon. As a first contribution, a control law is proposed, which is shown to guarantee global asymptotic stability of the counterclockwise circular motion around a fixed beacon, in the single-vehicle case. This turns out to be a useful property also in the multi-agent case, because each vehicle tries to rotate around the beacon in the same direction of rotation. Then, the control law is suitably modified to cope with the multi-vehicle case. Equilibrium configurations of the multi-vehicle system under the proposed control law are discussed and sufficient conditions for local asymptotic stability are derived. Sensory limitations are explicitly taken into account; in particular: i) each agent can perceive only vehicles lying in a limited visibility region; ii) a vehicle cannot measure the orientation of another vehicle, but only its relative distance; iii) vehicles are indistinguishable. Finally, simulation results are presented to show the effectiveness of the proposed control law in the multi-vehicle case.

The paper is organized as follows. In Section II, the control law is formulated for the single-vehicle case. Global asymptotic stability of the counterclockwise circular motion around a fixed beacon is proved. Section III concerns the multi-vehicle scenario: the modified control law is introduced and the resulting equilibrium configurations are studied. Sufficient conditions for local stability are given. Simulation results are provided in Section IV, while some concluding remarks and future research directions are outlined in Section V.

II. Control law for a single vehicle

Consider the planar unicycle model

$$\begin{aligned} \dot{x}(t) &= v\cos\theta(t) && (1)\\ \dot{y}(t) &= v\sin\theta(t) && (2)\\ \dot{\theta}(t) &= u(t); && (3) \end{aligned}$$

where $[x\ y\ \theta] \in \mathbb{R}^2 \times [-\pi, \pi)$ represents the vehicle pose, v is the forward speed (assumed to be constant) and $u(t)$ is the angular speed, which plays the role of control input.
The following control law, based on the vehicle relative pose with respect to a reference *beacon*, is proposed

$$u(t) = k \cdot g(\rho(t)) \cdot \alpha_{dist}(\rho(t), \gamma(t)) \qquad (4)$$

with

$$g(\rho) = ln\Big(\frac{(c-1)\cdot\rho + \rho_0}{c\cdot\rho_0}\Big) \qquad (5)$$

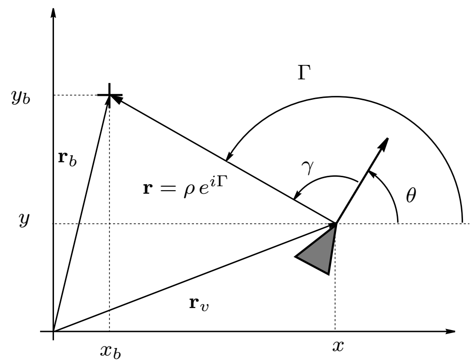

Fig. 1. Single vehicle (triangle) and beacon (cross).

and

$$\alpha_{dist}(\rho,\gamma) = \begin{cases} \gamma & \rho > 0 \quad \wedge \quad 0 \le \gamma \le \psi \\ \gamma - 2\pi & \rho > 0 \quad \wedge \quad \psi < \gamma < 2\pi \\ 0 & \rho = 0 \end{cases} . \quad (6)$$

In (4)-(6), ρ is the distance between the vehicle position $\mathbf{r}_v$=$[x\ y]'$ and the beacon position $\mathbf{r}_b = [x_b\ y_b]'$; $\gamma \in [0, 2\pi)$ represents the angular distance between the heading of the vehicle and the direction of the beacon (see Fig. 1); $k > 0$, $c > 1$, $\rho_0 > 0$ and $\psi \in (\frac{3}{2}\pi, 2\pi)$ are given constants.

Remark 1: The terms in equation (4) have different motivations. The term $g(\rho)$ in (5) assures that the control law steers the vehicle towards the beacon if $\rho \ge \rho_0$ and steers it away from the beacon if $\rho \le \rho_0$. The term α_{dist} in (6) is chosen to privilege the counterclockwise rotation with respect to the clockwise one, and it is critical for stability analysis. The threshold ψ is introduced so that, when ρ is large and γ is close to 2π, the vehicle goes straight towards the beacon instead of making useless circular motions (which would slow down convergence, especially in the multi-vehicle case). The choice of $\psi > \frac{3}{2}\pi$ is necessary to guarantee a unique direction of rotation about the beacon (as it will be shown in the following).

Let us introduce the following change of variables (see [6])

$$\mathbf{r} = \mathbf{r}_b - \mathbf{r}_v = \rho\, e^{i\Gamma} \quad (7)$$
$$\rho = \sqrt{(x - x_b)^2 + (y - y_b)^2} \quad (8)$$
$$\gamma = (\Gamma - \theta)\mathrm{mod}(2\pi) \quad (9)$$

where $\Gamma \in [0, 2\pi)$ denotes the angular distance between $\mathbf{r}$ and the x-axis (see Fig. 1). By differentiating (7) with respect to time, one obtains

$$\dot{\mathbf{r}} = \dot{\rho}\, e^{i\Gamma} + i\rho\,\dot{\Gamma} e^{i\Gamma} \ . \quad (10)$$

Since, by using (9), $\dot{\mathbf{r}} = -v\, e^{i\theta} = -v\, e^{-i\gamma}\, e^{i\Gamma}$, one has that for $\rho \neq 0$

$$\dot{\rho} = -v\, \cos\gamma \quad (11)$$
$$\dot{\Gamma} = \frac{v}{\rho}\, \sin\gamma \ . \quad (12)$$

By differentiating (9) with respect to time, and using (4)-(6), one gets

$$\begin{aligned} \dot{\gamma} &= \dot{\Gamma} - \dot{\theta} \\ &= \begin{cases} \frac{v}{\rho}\, \sin\gamma - k\, g(\rho)\, \gamma & \text{if} \quad 0 \le \gamma \le \psi \\ \frac{v}{\rho}\, \sin\gamma - k\, g(\rho)\, (\gamma - 2\pi) & \text{if} \quad \psi < \gamma < 2\pi \end{cases} . \end{aligned} \quad (13)$$

Let us consider now the system

$$\begin{aligned} \dot{\rho} &= -v\, \cos(\gamma) \\ \dot{\gamma} &= \begin{cases} \frac{v}{\rho}\, \sin\gamma - k\, g(\rho)\, \gamma & \text{if} \quad 0 \le \gamma \le \psi \\ \frac{v}{\rho}\, \sin\gamma - k\, g(\rho)\, (\gamma - 2\pi) & \text{if} \quad \psi < \gamma < 2\pi \end{cases} . \end{aligned} \quad (14)$$

The first aim is to guarantee that (14) has a unique equilibrium point, corresponding to counterclockwise rotation of the vehicle around the beacon. To this end, let us select the parameters v, k, c, ρ_0 so that

$$\min_{\rho}\ \rho\, g(\rho) \ > \ -\frac{2\, v}{3\, \pi\, k}. \quad (15)$$

This choice guarantees that for $\gamma = \frac{3}{2}\pi$ it holds that $\dot{\gamma} < 0$, i.e. clockwise rotation is not an equilibrium for system (14), or equivalently clockwise rotation is not a limit cycle for the system (1)-(6).

Let $\mathcal{D} \equiv \mathbb{R}_{++} \times (0, 2\pi)$, where $\mathbb{R}_{++}$ denotes the set of strictly positive real numbers. The following result is straightforward.

Proposition 1: The point $p_e = \begin{bmatrix} \rho_e \\ \frac{\pi}{2} \end{bmatrix}$ where ρ_e is such that:

$$\frac{v}{\rho_e} - k \cdot g(\rho_e) \cdot \frac{\pi}{2} = 0 \quad (16)$$

is the only equilibrium of system (14), for $(\rho, \gamma) \in \mathcal{D}$.

The consequence of Proposition 1 is that counterclockwise circular motion with radius ρ_e and angular velocity $\dot{\Gamma} = \frac{v}{\rho_e}$ is a limit cycle for system (1)-(6).

In order to perform stability analysis of p_e, let us introduce the following Lyapunov function

$$V(\rho,\gamma) = \int_{\rho_e}^{\rho} A(\hat{\rho}) d\hat{\rho} + \int_{\frac{\pi}{2}}^{\gamma} B(\hat{\gamma}) d\hat{\gamma} \quad (17)$$

where

$$B(\gamma) = \begin{cases} -\frac{\cos\gamma}{\gamma} & \text{if} \quad 0 < \gamma \le \psi \\ -\frac{\cos\gamma}{\gamma - 2\pi} & \text{if} \quad \psi < \gamma < 2\pi \end{cases} \quad (18)$$

and

$$A(\rho) = \frac{2}{\pi v}\Big(k\, g(\rho)\, \frac{\pi}{2} - \frac{v}{\rho}\Big). \quad (19)$$

Hence

$$\dot{V}(\rho,\gamma) = \begin{cases} \frac{v}{\rho} \cdot \cos\gamma \cdot \left(\frac{2}{\pi} - \frac{\sin\gamma}{\gamma}\right) & \text{if} \quad 0 < \gamma \le \psi \\ \frac{v}{\rho} \cdot \cos\gamma \cdot \left(\frac{2}{\pi} - \frac{\sin\gamma}{\gamma - 2\pi}\right) & \text{if} \quad \psi < \gamma < 2\pi \end{cases} .$$

Define the following sets:

$$\bar{\mathcal{D}} \equiv \mathbb{R}_{++} \times (0, \frac{3}{2}\pi], \quad (20)$$
$$\mathcal{K} \equiv \mathbb{R}_{++} \times (\psi, 2\pi), \quad (21)$$
$$\hat{\mathcal{D}} \equiv \mathcal{D} \setminus \bar{\mathcal{D}}. \quad (22)$$

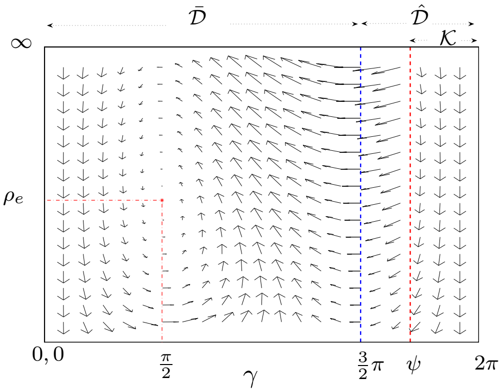

Fig. 2. Vector field (14) on $\mathcal{D}$.

It can be shown that $V(\rho,\gamma) \geq 0$, and $\dot{V}(\rho,\gamma) \leq 0$ for $(\rho,\gamma) \in \bar{\mathcal{D}}$, $\dot{V}(\rho,\gamma) < 0$ for $(\rho,\gamma) \in \mathcal{K}$. Moreover $V(\rho,\gamma) = 0$ only for $(\rho_e, \frac{\pi}{2})$ and $V(\rho,\gamma)$ is radially unbounded on $\mathcal{D}$ i.e.

$$\lim_{\rho\to 0} V(\rho,\gamma) = +\infty \quad \lim_{\rho\to\infty} V(\rho,\gamma) = +\infty$$
$$\lim_{\gamma\to 0} V(\rho,\gamma) = +\infty \quad \lim_{\gamma\to 2\pi} V(\rho,\gamma) = +\infty.$$

Since the vector field (14) is discontinuous, one cannot use directly the LaSalle's Invariance Principle to prove asymptotic stability of p_e on $\mathcal{D}$. Notice however that it can be shown that one solution always exists, in the Filippov's sense (see e.g. [8], [9]). Nevertheless, the Lyapunov function (17) will be useful to prove the main result, stated below.

Theorem 1: For the kinematic system (1)-(6), the counterclockwise circular motion around the beacon of fixed position $\mathbf{r}_b$, with rotational radius ρ_e defined in (16) and angular velocity $\frac{v}{\rho_e}$, is a globally asymptotically stable limit cycle.

In order to prove Theorem 1, two preliminary Lemmas are needed. First, it is proved that for any initial condition in $\hat{\mathcal{D}}$, there exists a finite time t^* such that $(\rho(t^*),\gamma(t^*)) \in \bar{\mathcal{D}}$ (Lemma 1). Then, Lemma 2 shows that, for initial vehicle poses outside $\mathcal{D}$ (i.e., when $\gamma = 0$ or $\rho = 0$), there exists a finite time $\hat{t}$ such that $(\rho(\hat{t}),\gamma(\hat{t})) \in \bar{\mathcal{D}}$. From these two lemmas, one can conclude that every trajectory will end up in $\bar{\mathcal{D}}$ in finite time (a phase portrait of vector field (14) is depicted in Figure 2). Finally, Theorem 1 will be proved using Lyapunov arguments in $\bar{\mathcal{D}}$.

Lemma 1: For any initial condition $(\rho_0,\gamma_0) \in \hat{\mathcal{D}}$, there exists $t^* > 0$ such that

$$(\rho(t^*),\gamma(t^*)) \in \bar{\mathcal{D}}. \tag{23}$$

Proof: Consider the following sets:

$$\hat{\mathcal{D}}_1 \equiv \mathbb{R}_{++} \times (\frac{3}{2}\pi, \beta]$$
$$\hat{\mathcal{D}}_2 \equiv \mathbb{R}_{++} \times (\beta, 2\pi)$$

where β is such that $\dot{\gamma} < -f < 0$ for any $(\rho,\gamma) \in \hat{\mathcal{D}}_1$. Notice that such a β can always be found because of (15). Observe that for any $(\rho,\gamma) \in \hat{\mathcal{D}}$, one has $\dot{\rho} < 0$ but, despite the discontinuity in (14), also

$$\lim_{\rho\to 0^+} \dot{\gamma}(\rho,\gamma) = -\infty \quad \forall \gamma \in (\tfrac{3}{2}\pi, 2\pi),$$

and hence the trajectories cannot leave the set $\hat{\mathcal{D}}$ through the line $\rho = 0$. Moreover, because $V(\rho,\gamma)$ is radially unbounded on $\mathcal{D}$ and $\dot{V}(\rho,\gamma) < 0$ on the set $\mathcal{K}$ in (21), then the trajectories cannot leave the set $\hat{\mathcal{D}}$ through the line $\gamma = 2\pi$. Now consider any initial condition $(\rho_0,\gamma_0) \in \hat{\mathcal{D}}_2$. In such set, one has

$$\dot{\rho} \leq -v \cos\beta < 0.$$

Since there cannot exist trajectories such that $\rho(t) = 0$ or $\gamma(t) = 2\pi$, as shown above, one can always find a time $t_1 \leq \frac{\rho_0}{v\cos\beta}$ such that $\gamma(t_1) = \beta$ and hence $(\rho(t_1),\gamma(t_1)) \in \hat{\mathcal{D}}_1$. Choose now any initial condition $(\rho_0,\gamma_0) \in \hat{\mathcal{D}}_1$. Since $\dot{\gamma} < -f$, and there cannot exist a trajectory such that $\rho(t) = 0$, one can always find a time $t_2 \leq \frac{\gamma_0 - \frac{3}{2}\pi}{f}$ such that $\gamma(t_2) = \frac{3}{2}\pi$ with $\rho(t_2) > 0$. Therefore, we have proved that for any initial condition in $\hat{\mathcal{D}}$, there exists a finite time t^* such that $(\rho(t^*),\gamma(t^*)) \in \bar{\mathcal{D}}$. ■

Now, let us consider all the initial vehicle poses such that the vehicle points towards the beacon, or the vehicle lies exactly on the beacon, i.e.

$$\begin{aligned} \mathcal{B} \equiv\ & \{(\mathbf{r}_b, \mathbf{r}_v(0), \theta(0)) : \gamma = 0,\ 0 < \rho < \infty\} \\ & \cup \{(\mathbf{r}_b, \mathbf{r}_v(0), \theta(0)) : \rho = 0\}. \end{aligned} \tag{24}$$

Lemma 2: For any trajectory of system (1)-(6) with initial conditions in $\mathcal{B}$, there exists a finite time $\hat{t}$ such that $(\rho(\hat{t}),\gamma(\hat{t})) \in \bar{\mathcal{D}}$.

Proof: Define the following sets of initial conditions

$$\mathcal{B}_1 = \{(\mathbf{r}_b, \mathbf{r}_v(0), \theta(0)) : \gamma = 0,\ 0 < \rho < \infty\},$$
$$\mathcal{B}_2 = \{(\mathbf{r}_b, \mathbf{r}_v(0), \theta(0)) : \rho = 0\}.$$

Consider first $(\mathbf{r}_b, \mathbf{r}_v(0), \theta(0)) \in \mathcal{B}_1$. Then, system (14) boils down to

$$\dot{\rho}(t) = -v$$
$$\dot{\gamma}(t) = 0$$

$\forall t \in [0, \bar{t})$ where $\bar{t} = \frac{\rho(0)}{v}$. Hence the vehicle proceeds straight towards the beacon until it reaches it, i.e. $\rho(\bar{t}) = 0$ and hence $(\mathbf{r}_b, \mathbf{r}_v(\bar{t}), \theta(\bar{t})) \in \mathcal{B}_2$.

Consider now an initial condition $(\mathbf{r}_b, \mathbf{r}_v(0), \theta(0)) \in \mathcal{B}_2$ (notice that in this case γ is not defined). We want to prove that in finite time $(\rho(t),\gamma(t)) \in \bar{\mathcal{D}}$. W.l.o.g. set $\mathbf{r}_b = \mathbf{r}_v(0) = [0,0]'$ and $\theta(0) = 0$. Observe that system (1)-(6) doesn't have any equilibrium point, and that $\dot{\theta}$ obtained from (3)-(4) is bounded in compact sets. This means that there exists $\delta > 0$ such that $|\theta(t)| \leq M\,\delta =: \epsilon$, $\forall t \leq \delta$ (one can choose e.g., $M = k\,\ln(c)\,\psi$). Hence, it follows that

$$\begin{bmatrix} v\,\delta\,\cos\epsilon \\ 0 \end{bmatrix} \preceq |\mathbf{r}_v(\delta)| \preceq \begin{bmatrix} v\,\delta \\ v\,\delta\,\sin\epsilon \end{bmatrix}, \tag{25}$$

where $|\cdot|$ and $\preceq$ have to be interpreted as componentwise operators. By geometric arguments it can be shown that

$$\begin{aligned} v\,\delta\,\cos\epsilon &\leq \rho(\delta) \leq v\,\delta \\ \pi - 2\epsilon &\leq \gamma(\delta) \leq \pi + 2\epsilon \end{aligned}$$

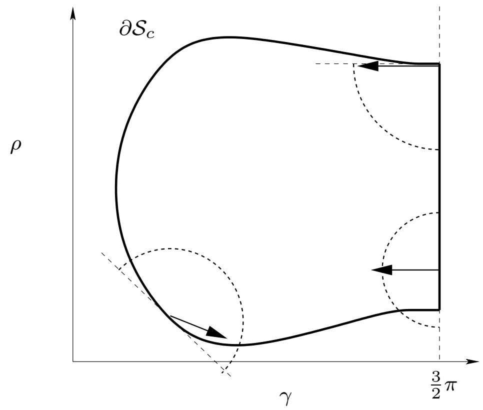

Fig. 3. Examples of contingent cones for a set $\mathcal{S}_c$. The dashed circular sectors represent the contingent cones associated to different points on $\partial\mathcal{S}_c$. The arrows represent the corresponding vector field (26).

which means $(\rho(\delta), \gamma(\delta)) \in \bar{\mathcal{D}}$. This concludes the proof. ■

Now Theorem 1 can be proved.

Proof: From Lemmas 1-2 it follows that for any initial condition $(\mathbf{r}_b, \mathbf{r}_v(0), \theta(0)) \in \mathbb{R}^2 \times \mathbb{R}^2 \times [0, 2\pi)$, there exists a finite time $t^* \geq 0$ such that $(\rho(t^*), \gamma(t^*)) \in \bar{\mathcal{D}}$. Now we want to prove that any trajectory starting in $\bar{\mathcal{D}}$ converges to the equilibrium p_e defined in Proposition 1. Notice that in $\bar{\mathcal{D}}$ system (14) boils down to

$$\begin{array}{rcl} \dot{\rho} & = & -v\,\cos\gamma \\ \dot{\gamma} & = & \frac{v}{\rho}\,\sin\gamma - k\,g(\rho)\,\gamma. \end{array} \tag{26}$$

Consider any initial condition $(\rho_0, \gamma_0) \in \bar{\mathcal{D}}$. Define $c = V(\rho_0, \gamma_0)$ and the set

$$\mathcal{S}_c \equiv \big\{(\rho, \gamma) \in \bar{D} : V(\rho, \gamma) \leq c\big\}. \tag{27}$$

Since $V(\rho, \gamma)$ is radially unbounded, the set $\mathcal{S}_c$ is compact and its boundary has the following form

$$\begin{array}{rl} \partial\mathcal{S}_c \equiv \big\{(\rho, \gamma) : & (V(\rho, \gamma) = c \wedge \gamma < \frac{3}{2}\pi) \vee \\ & (V(\rho, \gamma) \leq c \wedge \gamma = \frac{3}{2}\pi)\big\}. \end{array} \tag{28}$$

We want to show that the set $\mathcal{S}_c$ is a *viability domain* for the system (26), i.e. the vector field always points inside, or is tangent to, the *contingent cone* to any point on $\partial\mathcal{S}_c$ (see Figure 3, and [10, p. 25-26] for a rigorous definition).

Consider, if there exists, any $(\rho, \gamma) \in \partial\mathcal{S}_c$ such that

$$\gamma = \tfrac{3}{2}\pi \quad V(\rho, \gamma) < c.$$

Because of (15) the vector field defined by system (26) is of the form

$$\left[\begin{array}{c} \dot{\rho} \\ \dot{\gamma} \end{array}\right] = \left[\begin{array}{c} 0 \\ -\alpha \end{array}\right] \tag{29}$$

with $\alpha > 0$. Hence, it points inside the contingent cone.

Consider now $(\rho, \gamma) \in \partial\mathcal{S}_c$ such that

$$\gamma < \tfrac{3}{2}\pi \quad V(\rho, \gamma) = c.$$

Since for such (ρ, γ) one has $\dot{V}(\rho, \gamma) < 0$, the vector field points inside the contingent cone to $\mathcal{S}_c$.

Finally consider, if there exists, any $(\rho, \gamma) \in \partial\mathcal{S}_c$ such that

$$\gamma = \tfrac{3}{2}\pi \quad V(\rho, \gamma) = c.$$

Notice that for such (ρ, γ), one has $\nabla V(\rho, \gamma) = [\beta, 0]$, with $\beta \in \mathbb{R}$. Hence, one of the two edges of the contingent cone to $\partial\mathcal{S}_c$ is orthogonal to the line $\gamma = \frac{3}{2}\pi$ (see Figure 3). Again, from (26) one has that the vector field is of the form (29) and hence it is tangent to the contingent cone.

Now, notice that the vector field (26) is Lipschitz on $\mathcal{S}_c$. Hence, by applying Nagumo theorem (see e.g., [10, Theorem 1.2.4, p. 28]), for any $(\rho_0, \gamma_0) \in \mathcal{S}_c$ there exists a unique solution for $t \in [0, \infty]$, and such solution will not leave $\mathcal{S}_c$. In other words, $\mathcal{S}_c$ is a positively invariant set with respect to system (26).

By recalling that $\dot{V}(\rho, \gamma) \leq 0$, $\forall(\rho, \gamma) \in \bar{\mathcal{D}}$, one can apply LaSalle's Invariance Principle (see e.g. [11]) to conclude that the trajectories starting in $\mathcal{S}_c$ converge asymptotically to the largest invariant set $\mathcal{M}$ such that

$$\mathcal{M} \subseteq E \equiv \{(\rho, \gamma) \in \mathcal{S}_c : \dot{V}(\rho, \gamma) = 0\}.$$

It is trivial to show that, for any $c \geq 0$, the set $\mathcal{M}$ contains only the equilibrium point p_e. Being the choice of $(\rho_0, \gamma_0) \in \bar{\mathcal{D}}$ arbitrary, convergence to p_e occurs for any trajectory starting in $\bar{\mathcal{D}}$. Because the equilibrium point p_e corresponds to counterclockwise circular motion around the beacon $\mathbf{r}_b$ with radius ρ_e, it can be concluded that such motion is a globally asymptotically stable limit cycle for the system (1)-(6). ■

Remark 2: The stability analysis of this section holds for a larger class of functions $g(\rho)$, than the one proposed in (5). In particular for any locally Lipschitz $g(\rho)$ such that

- the inequality (15) holds
- $\exists!\ \rho_e$ s.t $A(\rho_e) = 0$
- $A(\rho) > 0$ for $\rho > \rho_e$
- $A(\rho) < 0$ for $\rho < \rho_e$,

with $A(\rho)$ defined in (19), the counterclockwise circular motion is globally asymptotically stable for the system (1)-(6). It is trivial to show that the function (5) belongs to this class. Moreover notice that global stability is preserved also using simpler functions, e.g. $g(\rho) = \text{constant} > 0$.

III. Multi-vehicle systems

In this section the control law (4) is modified in order to deal with a multi-vehicle scenario. Consider a group of n agents whose motion is described by the kinematic equations

$$\dot{x}_i(t) = v\,\cos\theta_i(t) \tag{30}$$

$$\dot{y}_i(t) = v\,\sin\theta_i(t) \tag{31}$$

$$\dot{\theta}_i(t) = u_i(t), \tag{32}$$

with $i = 1 \ldots n$. Let: ρ_i and γ_i be defined as in Section II; ρ_{ij} and γ_{ij} denote respectively the linear and angular distance between vehicle i and vehicle j (see Figure 4); $g(\rho, c, \rho_0)$ be equal to $g(\rho)$ in (5). In the control input $u_i(t)$ a new additive term is introduced which depends on the interaction between the i-th vehicle and any other perceived vehicle j

$$u_i(t) = f_{ib}(\rho_i, \gamma_i) + \sum_{\substack{j \neq i \\ j \in \mathcal{N}_i}} f_{ij}(\rho_{ij}, \gamma_{ij}) \tag{33}$$

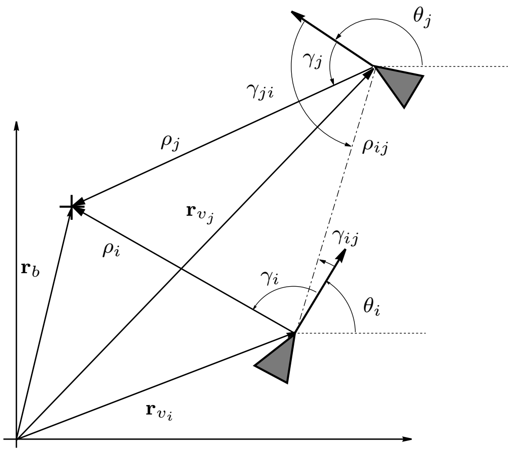

Fig. 4. Two vehicles (triangles) and a beacon (cross).

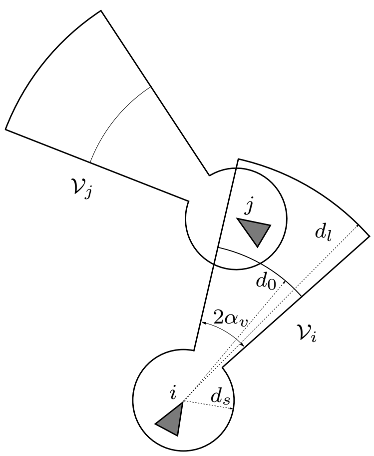

Fig. 5. Visibility region of i-th and j-th vehicle.

where f_{ib} is the same as in the right hand side of (4), i.e.

$$f_{ib}(\rho_i, \gamma_i) = k_b \cdot g(\rho_i, c_b, \rho_0) \cdot \alpha_{dist}(\rho_i, \gamma_i), \qquad (34)$$

while

$$f_{ij}(\rho_{ij}, \gamma_{ij}) = k_v \cdot g(\rho_{ij}, c_v, d_0) \cdot \beta_{dist}(\gamma_{ij}), \qquad (35)$$

with $k_v > 0$, $c_v > 1$, $d_0 > 0$ and

$$\beta_{dist}(\gamma_{ij}) = \begin{cases} \gamma_{ij} & 0 \le \gamma_{ij} \le \pi \\ \gamma_{ij} - 2\pi & \pi < \gamma_{ij} < 2\pi \end{cases} . \qquad (36)$$

The set $\mathcal{N}_i$ contains the indexes of the vehicles lying inside the visibility region $\mathcal{V}_i$ associated with the i-th vehicle. In this paper, the visibility region has been chosen as the union of the following two sets (see Figure 5):

- Circular sector of ray d_l and angular amplitude $2\alpha_v$, centered at the vehicle pose and orientation. It represents long range sensor with limited angular visibility (e.g., a laser range finder).
- Circular region around the vehicle of radius d_s, which represents a proximity sensor (e.g., a ring of sonar).

Remark 3: The intuitive motivation of such a control law relies in the fact that each agent i is driven by the term $f_{ib}(\cdot)$ towards the counterclockwise circular motion about the beacon, while the terms $f_{ij}(\cdot)$ (and the visibility regions $\mathcal{V}_i$) favour collision free trajectories trying to keep distance $\rho_{ij} = d_0$ for all the agents $j \in \mathcal{N}_i$. This follows intuitively from the fact that vehicle i is attracted by any vehicle $j \in \mathcal{N}_i$ if $\rho_{ij} > d_0$, and repulsed if $\rho_{ij} < d_0$. The expected result of such combined actions is that the agents reach the counterclockwise circular motion in a number of platoons, in which the distances between consecutive vehicles is d_0. As it will be shown in Section IV, this is confirmed by simulations (see for example Figure 8).

In the following, local stability analysis of system (30)-(32) under the control law (33)-(36), is presented.

A. Equilibrium configurations

From Section II and by using a coordinate transformation similar to the one adopted in [2], one obtains the equations

$$\dot{\rho}_i = -v \cos\gamma_i \qquad (37)$$

$$\dot{\gamma}_i = \frac{v}{\rho_i} \sin\gamma_i - u_i \qquad (38)$$

$$\dot{\rho}_{ij} = -v\,(\cos\gamma_{ij} + \cos\gamma_{ji}) \qquad (39)$$

$$\dot{\gamma}_{ij} = \frac{v}{\rho_{ij}}\,(\sin\gamma_{ij} + \sin\gamma_{ji}) - u_i \qquad (40)$$

$\forall i, j = 1 \dots n$, $j \neq i$, and u_i defined in (33). Notice that there are algebraic relationships between the state variables $\rho_i, \gamma_i, \rho_{ij}, \gamma_{ij}$, which must be taken into account in the stability analysis.
Let us choose the parameters d_0, d_l and the number of vehicles n so that

$$(n-1)\,\arcsin\left(\frac{d_0}{2\rho_e}\right) + \arcsin\left(\frac{d_l}{2\rho_e}\right) < \pi. \qquad (41)$$

This choice guarantees that the n vehicles can lie on a circle of radius ρ_e, with distance d_0 between two consecutive vehicles and distance longer than d_l between the first and the last.

Proposition 2: Every configuration of n vehicles in counterclockwise circular motion about a fixed beacon, with rotational ray $\rho_i = \rho_e$ defined in (16), and $\rho_{ij} = d_0$ $\forall i = 1 \dots n$ and $\forall j \in \mathcal{N}_i$, corresponds to an equilibrium point of system (37)-(40).

Proof: First, notice that by assumption (41), there is at least one configuration that satisfies the statement of the proposition. The counterclockwise circular motion implies $\gamma_i = \frac{\pi}{2}$, and hence $\dot{\rho}_i = 0$. Now, notice that $\rho_{ij} = d_0$ for any $j \in \mathcal{N}_i$ implies that $f_{ij}(\cdot) = 0$. Hence u_i in (33) is equal to (4). From (16), it can be concluded that for $\rho_i = \rho_e$ one has $\dot{\gamma}_i = 0$. If all the vehicles lie on the same circle of radius ρ_e, with the same direction of rotation, by trivial geometric considerations it can be shown that $\gamma_{ij} + \gamma_{ji} = \pi$ and $\min\{\gamma_{ij}, \gamma_{ji}\} = \arcsin\left(\frac{\rho_{ij}}{2\rho_e}\right)$. Hence $\dot{\rho}_{ij} = 0$ and, by exploiting (16) again

$$\dot{\gamma}_{ij} = \frac{v}{\rho_{ij}} \cdot 2\sin\gamma_{ij} - \frac{v}{\rho_e} = 0.$$

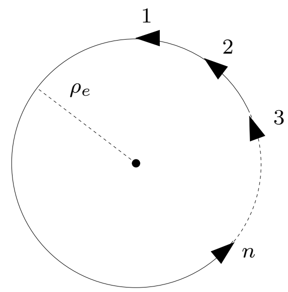

Fig. 6. A possible equilibrium configuration of n vehicles: $\mathcal{N}_i = \{i-1\}$ and $\rho_{i(i-1)} = d_0$ for $i = 2, \ldots, n$, while $\mathcal{N}_1$ is empty.

which concludes the proof. ■

Remark 4: Consider visibility regions with $d_s < d_0$ and $\alpha_v \leq \pi/2$ (typical for range finders). Hence, the condition $\rho_{ij} = d_0$ $\forall i = 1 \ldots n$ and $\forall j \in \mathcal{N}_i$ in Proposition 2 implies that, when lying on the circle of radius ρ_e, each vehicle perceives at most one vehicle, i.e. card$(\mathcal{N}_i) \in \{0, 1\}$. Moreover, due to assumption (41), there is at least one vehicle that does not perceive the others. If there are q vehicles with card$(\mathcal{N}_i) = 0$ and $n - q$ vehicles with card$(\mathcal{N}_i) = 1$, the equilibrium configuration is made of q separate platoons. The limit cases are obviously $q = 1$ (a unique platoon) and $q = n$ (n vehicles rotating independently around the beacon).

B. Local stability analysis

Let us choose $d_s < d_0$ and $\alpha_v \leq \pi/2$, so that card$(\mathcal{N}_i) \in \{0, 1\}$ in the equilibrium configurations defined by Proposition 2. W.l.o.g. consider n vehicles in counter-clockwise circular motion about a beacon and renumber them as in Figure 6. The equilibrium point defined by Proposition 2 is therefore

$$\begin{array}{lll} \rho_i = \rho_e & \gamma_i = \frac{\pi}{2} & i = 1 \ldots n \\ \gamma_{(i-1)i} = \frac{\pi}{2} + \arccos(\frac{d_0}{2\rho_e}) & & i = 2 \ldots n. \end{array} \tag{42}$$

Being card$(\mathcal{N}_1) = 0$ and card$(\mathcal{N}_i) = 1$ for $i \geq 2$, the kinematic of the i-th vehicle is locally affected only by the position of the beacon and that of vehicle $i-1$, except for vehicle 1 whose kinematic is locally determined only by the beacon position. We make the assumptions that there is a neighborhood of the equilibrium configuration in which the sets $\mathcal{N}_i$ does not change (this can be seen as a further mild constraint on the size of the visibility region, i.e. $\arcsin(\frac{d_l}{2\rho_e}) < 2\arcsin(\frac{d_0}{2\rho_e})$).
The total kinematic system is described by the equations

$$\dot{\rho}_1 = -v \cos\gamma_1 \tag{43}$$
$$\dot{\gamma}_1 = \frac{v}{\rho_1} \sin\gamma_1 - u_1 \tag{44}$$
$$\dot{\rho}_i = -v \cos\gamma_i \tag{45}$$
$$\dot{\gamma}_i = \frac{v}{\rho_i} \sin\gamma_i - u_i \tag{46}$$
$$\dot{\gamma}_{(i-1)i} = \frac{v}{\rho_{(i-1)i}} (\sin\gamma_{(i-1)i} + \sin\gamma_{i(i-1)}) - u_{i-1} \tag{47}$$

for $i = 2 \ldots n$. The control inputs are given by $u_1 = f_{1b}$ and $u_i = f_{ib} + f_{i(i-1)}$ for $i \geq 2$. Notice that the $3n-1$ state variables in system (43)-(47) are sufficient to describe completely the n-vehicles system. Indeed, the remaining state variables in system (37)-(40) can be obtained via algebraic relationships form the above $3n - 1$ ones. In particular one has

$$\rho_{(i-1)i} = \rho_{(i-1)} \cos(\gamma_{(i-1)i} - \gamma_{(i-1)}) + \\ + \sqrt{\rho_i^2 - \rho_{(i-1)}^2 \sin^2(\gamma_{(i-1)i} - \gamma_{(i-1)})} \tag{48}$$

$$\gamma_{i(i-1)} = \gamma_i - \arcsin\left(\frac{\rho_{(i-1)}}{\rho_i} \sin(\gamma_{(i-1)i} - \gamma_{(i-1)})\right) \tag{49}$$

for $i = 2, \ldots, n$.
By linearizing system (43)-(47) around the equilibrium point (42), one gets a system of the form

$$\begin{bmatrix} \dot{\rho}_1 \\ \dot{\gamma}_1 \\ \dot{\rho}_2 \\ \dot{\gamma}_2 \\ \dot{\gamma}_{12} \\ \vdots \\ \dot{\rho}_n \\ \dot{\gamma}_n \\ \dot{\gamma}_{(n-1)n} \end{bmatrix} = \begin{bmatrix} A & 0 & \cdots & 0 \\ * & B & \ddots & \vdots \\ \vdots & \ddots & \ddots & 0 \\ * & \cdots & * & B \end{bmatrix} \cdot \begin{bmatrix} \rho_1 \\ \gamma_1 \\ \rho_2 \\ \gamma_2 \\ \gamma_{12} \\ \vdots \\ \rho_n \\ \gamma_n \\ \gamma_{(n-1)n} \end{bmatrix} \tag{50}$$

where $A \in \mathbb{R}^{2\times2}$ and $B \in \mathbb{R}^{3\times3}$. The eigenvalues of A are strictly negative; in fact the kinematic of vehicle 1 is decoupled by that of the other vehicles, and hence the stability analysis performed in Section II for the single vehicle case holds. Therefore, it is sufficient to show that matrix B is Hurwitz to guarantee local stability of system (43)-(47).

In order to compute the expression of matrix B, one has to take into account the dependence of the right hand side of (46) and (47) on $\rho_{(i-1)i}$ and $\gamma_{i(i-1)}$, which in turn depend on ρ_i, γ_i and $\gamma_{(i-1)i}$ via (48)-(49). Through some tedious calculations, it can be shown that matrix B has the form

$$\begin{bmatrix} 0 & v & 0 \\ -b_{21} & -b_{22} & b_{23} \\ -b_{31} & b_{32} & b_{33} \end{bmatrix} \tag{51}$$

where

$$\begin{aligned} b_{21} = {} & \tfrac{v}{\rho_e^2} + k_b \tfrac{c_b - 1}{(c_b-1)\rho_e + \rho_0} \tfrac{\pi}{2} + \\ & k_v \tfrac{c_v - 1}{c_v d_0} \left(\tfrac{\pi}{2} - \arccos(\tfrac{d_0}{2\rho_e})\right) \tfrac{2\rho_e}{d_0} \\ b_{22} = {} & \tfrac{2v}{\pi \rho_e} \\ b_{23} = {} & k_v \tfrac{c_v - 1}{c_v d_0} \sqrt{4\rho_e^2 - d_0^2} (\tfrac{\pi}{2} - \arccos(\tfrac{d_0}{2\rho_e})) \\ b_{31} = {} & \tfrac{v}{2\rho_e^2} \\ b_{32} = {} & \tfrac{v}{d_0} \sqrt{1 - \tfrac{d_0^2}{4\rho_e^2}} \\ b_{33} = {} & 0. \end{aligned}$$

By noticing that $b_{ij} \geq 0$, and applying the Routh-Hurwithz criterion to the characteristic polynomial of matrix B, it can be seen that the only condition that must be checked is $b_{22}(vb_{21} + b_{32}b_{23}) + vb_{31}b_{23} > 0$. Moreover it can be shown that the following inequality holds

$$b_{22}(vb_{21}+b_{32}b_{23})+vb_{31}b_{23} > \frac{v^2}{\rho_e^2}\left\{\frac{2v}{\pi\rho_e}+k_b\frac{c_b-1}{c_b}-\frac{1}{2}k_v\frac{c_v-1}{c_v}\right\}. \qquad (52)$$

Therefore, it suffices to enforce positivity of the right hand side in (52) to guarantee local asymptotic stability of the considered equilibrium. This holds for example whenever

$$\frac{k_v}{k_b} \leq 2\,\frac{c_v}{c_b}\,\frac{c_b-1}{c_v-1}\,.$$

On the other hand, (52) gives a guideline to find values of the parameters for which the considered equilibrium is unstable: examples can easily be found for $c_v = c_b$ and $k_v \gg k_b$, or for $k_v = k_b$ and $c_v \gg c_b$. This is in good agreement with intuition, as it basically says that the beacon-driven control term should not be excessively reduced with respect to the control input due to interaction with the other agents.

IV. Simulation results

In this section, simulation studies are provided for the multi-vehicle system (30)-(32) under the control law (33)-(36). In all the examples, the considered visibility region $\mathcal{V}_i$ has been chosen with $d_l = 12$, $\alpha_v = \frac{\pi}{4}$, $d_s = 3$. The control law parameters are set to: $\psi = \frac{7}{4}\pi$, $k_b = 0.07$, $c_b = 2$, $k_v = 0.1$, $c_v = 3$, $d_0 = 8$.

A 4-vehicle system with a static reference beacon is considered in Figure 7, with $v = 0.3$, $\rho_0 = 6$. It can be seen that the multi-vehicle system converges to a single-platoon formation, which satisfies Proposition 2 with $\rho_e \simeq 9.84$ given by (16).

A 8-vehicle system is considered in Figure 8. In this case, $v = 1$ and $\rho_0 = 10$. The equilibrium configuration reached by the multi-vehicle system consists of 3 separate platoons of cardinality 5, 2 and 1 respectively (i.e., $q = 3$ according to Remark 4), with radius $\rho_e \simeq 20.9$.

In Figure 9, the same control law has been applied to the case of 6 vehicles following a non-static beacon, to evaluate the tracking behavior of the multi-vehicle system. The beacon moves through four sequential way-points. A similar scenario was considered in [7]. In particular, the beacon trajectory is

$$\begin{array}{lll} \mathbf{r}_{b_1} = [0,0]' & \text{if} & t \leq 600 \\ \mathbf{r}_{b_2} = [100,0]' & \text{if} & 600 \leq t \leq 1200 \\ \mathbf{r}_{b_3} = [100,100]' & \text{if} & 1200 \leq t \leq 1800 \\ \mathbf{r}_{b_4} = [0,100]' & \text{if} & t \geq 1800 \end{array}$$

Notice that when the current target changes from $\mathbf{r}_{b_i}$ to $\mathbf{r}_{b_j}$, the vehicles move from a rotational configuration about $\mathbf{r}_{b_i}$ towards $\mathbf{r}_{b_j}$ in a sort of parallel motion, see Figure 9. The trajectories show that the configuration in rotational motion is reached for each way-point.

Repeated runs have been performed to analyze the role of the initial configuration of the multi-vehicle system. In Figure 10, the estimated convergence times for 100 simulations with random initial conditions are reported, for the 4-vehicle system considered above. The convergence test is based on the difference between the rotational radius of each vehicle and ρ_e (namely $|\rho_i(t) - \rho_e|$). All the simulations terminated with success.

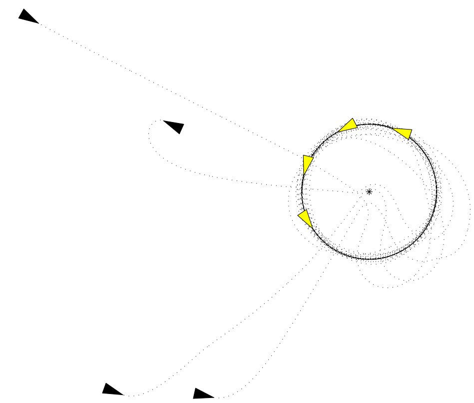

Fig. 7. A 4-vehicle scenario with static beacon (black triangles represent initial poses).

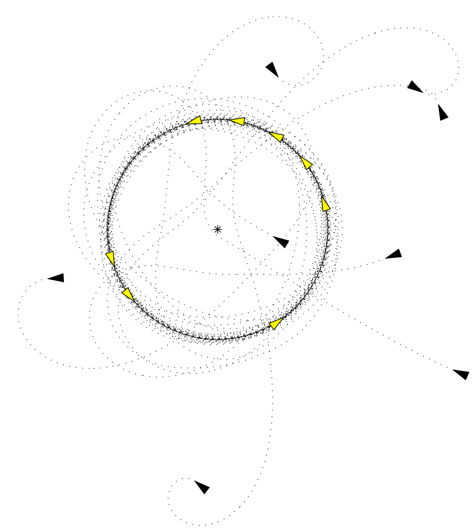

Fig. 8. A 8-vehicle scenario with static beacon.

The transient behavior of the multi-vehicle system is clearly affected by the choice of the control law parameters. In particular, the following aspects must be taken into account:

- The clockwise rotation about the beacon must *not* be an equilibrium point, i.e. the parameters have to verify inequality (15).
- The equilibrium radius ρ_e must be consistent with the number of vehicles and d_0. This means that the configuration of a single platoon in cyclic pursuit must be feasible with respect to inequality (41).
- The choice of k_v is influenced by a trade-off between collision avoidance and the effect of the beacon attraction. Indeed, notice that the multi-vehicle system with $k_v = 0$ is globally asymptotically stable by the trivial consideration that the overall system is the composition of globally asymptotically stable decoupled subsystems. This means that a possible source of instability could

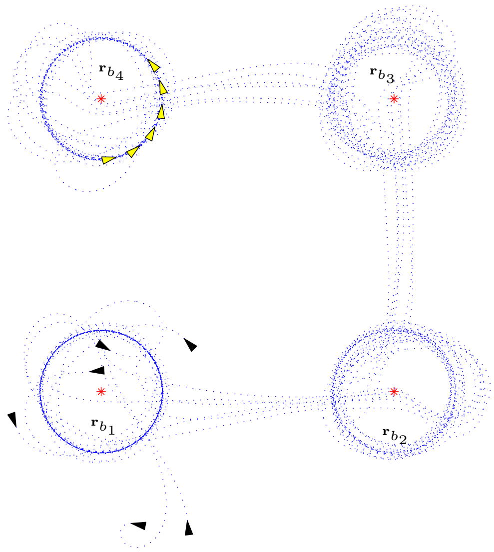

Fig. 9. A 6-vehicle team tracking a moving beacon (asterisks).

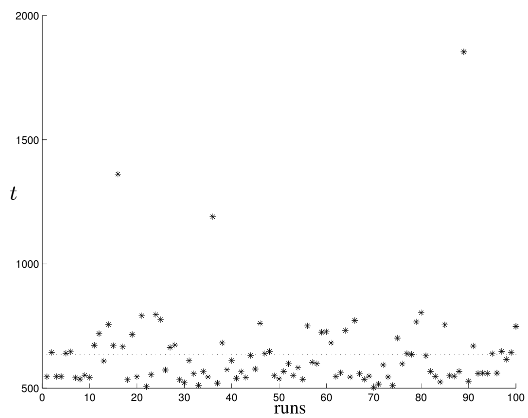

Fig. 10. Convergence times over 100 runs

come only from the cross terms in (35). In this respect, the choice of a "small" k_v is recommended for good performance in term of convergence time. On the contrary, a "large" k_v favours a safe collision-free motion.

V. Conclusions and future work

The main features of the control law proposed in this work are: i) it guarantees global stability in the single-vehicle case; ii) control parameters can be easily selected to achieve local stability of the equilibrium configurations of interest in the multi-vehicle scenario; iii) simulative studies show promising results in terms of convergence rate and tracking performance. With respect to similar approaches presented in the literature, quite restrictive assumptions have been removed, e.g.:

- total visibility is not required, i.e. the sensors perceive only the agents in the visibility regions $\mathcal{V}_i$;
- exteroceptive orientation measurements are not performed: each vehicle has to measure only distances to other vehicles lying in its visibility region;
- labeling of the vehicles is not required.

This aspects are critical for multi-vehicle systems with equipment limitations, hampering long range measurements or estimation of other vehicles orientation. Moreover, there is no need of smart communication protocols to identify vehicles or to exchange information, because the required measurements can be easily obtained from range sensors.

This work is still at a preliminary stage and several interesting developments can be foreseen. From a theoretical point of view, it would be desirable to provide sufficient conditions for the convergence of the multi-vehicle system to the desired equilibrium configurations. A deeper understanding of the role of the design parameters in the control law and how they affect the behavior of the multi-vehicle system would be useful. Moreover, the tracking performance in the presence of a moving beacon must be thoroughly investigated. In this respect, a nice feature of the proposed control law is that, when the beacon is faraway from the vehicles, each agent points straight towards it. Hence, a smooth transition between circular and parallel motion is expected.

VI. Acknowledgments

The authors would like to thank people at the Systems Control Group of the Department of Electrical and Computer Engineering, University of Toronto, for fruitful discussions, useful suggestions and comments, especially Prof. Bruce Francis, Prof. Mireille Broucke and Prof. Manfredi Maggiore.

References

[1] A. Jadbabaie, J. Lin, and A. S. Morse, "Coordination of groups of mobile autonomous agents using nearest neighbor rules," *IEEE Transactions on Automatic Control*, vol. 48, no. 6, pp. 988–1001, June 2003.

[2] J. A. Marshall, M. E. Broucke, and B. A. Francis, "Formations of vehicles in cyclic pursuit," *IEEE Transactions on Automatic Control*, vol. 49, no. 11, pp. 1963–1974, November 2004.

[3] N. E. Leonard and E. Fiorelli, "Virtual leaders, artificial potentials and coordinated control of groups," in *Proceedings of the IEEE Conference on Decision and Control*, Orlando, 2001, pp. 2968–2973.

[4] Z. Lin, M. E. Broucke, and B. A. Francis, "Local control strategies for groups of mobile autonomous agents," *IEEE Transactions on Automatic Control*, vol. 49, no. 4, pp. 622–629, April 2004.

[5] R. Sepulchre, D. Paley, and N. E. Leonard, "Collective motion and oscillator syncrhronization," in *Proc. Block Island Workshop on Cooperative Control*, V. Kumar, N. Leonard, and A. Morse, Eds., June 2003.

[6] E. W. Justh and P. S. Krishnaprasad, "Equilibria and steering laws for planar formations," *Systems and Control Letters*, vol. 52, pp. 25–38, 2004.

[7] D. Paley, N. E. Leonard, and R. Sepulchre, "Collective motion: bistability and trajectory tracking," in *Proceedings of the IEEE Conference on Decision and Control*, Nassau, Bahamas, 2004, pp. 1932–1936.

[8] A. Filippov, *Differential Equations with Discontinuous Righthand Sides*. Kluwer Academic Publisher, 1988.

[9] J. P. Aubin and A. Cellina, *Differential Inclusions*. Springer-Verlag Berlin Heidelberg New York Tokyo, 1984.

[10] J. P. Aubin, *Viability theory*. Birkhauser, 1991.

[11] H. Khalil, *Nonlinear Systems*. New York: Macmillan Publishing Co., 1992.